ELSEVIER

Organic Electronics 3 (2002) 15–21

Organic Electronics

www.elsevier.com/locate/orgel

The electronic structure of TPD films grown by different methods

E.Z. Kurmaev [a,*], K. Endo [b], T. Ida [b], T. Otsuka [b], S.Y. Kim [c], G.S. Chang [c], A. Moewes [d], N.Y. Kim [c], C.N. Whang [c], D.L. Ederer [e]

[a] *Institute of Metal Physics, Russian Academy of Sciences-Ural Division, 620219 Yekaterinburg GSP-170, Russia*
[b] *Department of Chemistry, Faculty of Science, Kanazawa University, Kakuma-machi, Kanazawa 920-1192, Japan*
[c] *Atomic-Scale Surface Science Research Center and Department of Physics, Yonsei University, Seoul 120-749, South Korea*
[d] *Department of Physics and Engineering Physics, University of Saskatchewan, 116 Science Place, Saskatoon, SK, Canada, S7N 5E2*
[e] *Department of Physics, Tulane University, New Orleans, LA 70118, USA*

Received 9 March 2001; received in revised form 18 August 2001; accepted 23 November 2001

Abstract

We present X-ray photoelectron spectra and X-ray emission spectra of *N*,*N*′-bis(3-methylphenyl)-*N*,*N*′-diphenyl-1,1′-biphenyl-4,4′-diamine (TPD) films excited with synchrotron radiation. The measurements are compared with density-functional theory calculations performed for a TPD monomer and the electronic structure of this material is discussed in detail. The TPD films studied in this work were prepared by ionized and neutral cluster beam deposition (ICBD and NCBD, respectively) as well as by thermal evaporation. X-ray fluorescence measurements show that the ICBD technique provides the most promising way of preparing high quality TPD films with strong electroluminescence. C–N bonds in the TPD structure are destroyed under NCBD as well as under thermal evaporation.

Keywords: Organic light-emitting diodes; Electroluminescence; Electronic structure; Density-functional theory; X-ray photoelectron spectra; X-ray emission spectra

1. Introduction

Multilayered polymeric [1–3] and molecular thin films [4–9] have attracted interest as organic light-emitting diodes (OLEDs) [10,11]. One of the promising candidates is the tris-(8-hydroxyquinoline) aluminum (Alq_3)/*N*,*N*′-di-(3-methylphenyl)-*N*,*N*′diphenyl-bis(3-methyl phenyl)-1,1′-biphenyl-4,4′-diamine (TPD) multilayered film. Alq_3 and TPD layers have been known to play a role in the light-emitting process as light-emitting layer and hole transport layer as well as in terms of electron transport. In order to understand the light-emitting mechanism of Alq_3/TPD multilayers, it is essential to study the characteristics of each layer. The ionized cluster beam deposition (ICBD) method has been found to be promising for obtaining sharp interface, high packing density, and smooth surface [12]. In this study, we applied the

* Corresponding author. Tel.: +7-343-27-44183; fax: +7-343-27-45244.
E-mail address: kurmaev@ifmlrs.uran.ru (E.Z. Kurmaev).

1566-1199/02/$ - see front matter
PII: S1566-1199(01)00026-X

ICBD method to grow the TPD film with a smooth surface and a well-defined molecular bonding. For comparison the TPD films were also prepared by neutral cluster beam deposition (NCBD) and by thermal evaporation. X-ray fluorescence measurements were used for the characterization of these films. It is shown that preparation of the films with the ICBD technique provides the best way for obtaining high quality TPD films, with strong electroluminescence (EL). In the case of preparation by NCBD or thermal evaporation, some bonds between carbon (C) and nitrogen (N) are broken in the TPD structure.

In this work, we demonstrate that X-ray photoelectron and emission spectroscopies are powerful tools for providing precise information on the electronic states of film substances. These experimental electron spectra of the substance are directly linked to the theoretical results of the electronic states as obtained by density-functional theory (DFT) calculations using model molecules. Here, we show that theoretical valence X-ray photoelectron and emission spectra for TPD obtained by deMon (DFT) calculations [13] using the model molecule are in a good accordance with the experiments to obtain valence X-ray photoelectron spectra (XPS) and C and N Kα X-ray emission spectra (XES).

2. Experiment

Fig. 1 shows the structure of TPD [15] which contains phenyl rings linked by N atoms and side CH_3 groups. The TPD films were prepared at room temperature on indium-tin-oxide (ITO) glasses by the ICBD and NCBD method respectively [12,14]. We can divide the ICB equipment into four parts. First, the crucible part which is used to dissolve the material, and to form molecule clusters. Second, the electron-gun part which is to ionize the molecule clusters. Third, the acceleration part which is used to accelerate the ionized molecule clusters. Fourth, the substrate holder upon which the molecule clusters are deposited. Thin films are obtained by the following method. First of all, the materials are loaded into crucibles, and heated to a suitable temperature. The molecular clusters are made by adiabatic expansion, and then they are ionized by electrons from the electron gun. The ionized clusters are accelerated by the electric field between crucible and substrate in case of ICBD, to obtain a thin film. During the ICBD process, the acceleration voltage was fixed at 800 V. TPD films deposited by thermal evaporation was also prepared for comparison to the ICBD method. During the thermal evaporation, the crucible was heated to 140 °C. The thickness of the TPD was monitored by a crystal oscillator to be about 50 nm and the deposition rates were fixed at 6 nm/min. The total pressure during the process was in the low 10^{-7} Torr range.

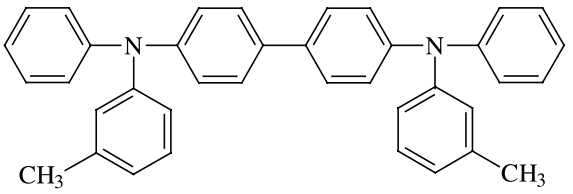

Fig. 1. The schematic diagram of TPD structure.

The C and N Kα ($2p \rightarrow 1s$ transition) XES were taken at the Advanced Light Source (Beamline 8.0), employing the University of Tennessee's soft X-ray fluorescence (SXF) endstation [16]. Photons with an energy of 300 eV, well above the C K edge and with an energy of 430 eV, well above the N K edge were delivered to the endstation via the beamline's 89-period, 5-cm undulator insertion device and spherical grating monochromator. The C and N Kα spectra were obtained in first order with a 600 lines/mm, 10 m radius grating providing an energy resolution of 0.3–0.4 eV. The C and N Kα emission spectra were calibrated with a reference sample of highly oriented pyrographite and hexagonal boron nitride, respectively.

We measured the valence band spectra of TPD films by using X-ray photoelectron spectroscopy (XPS) at Atomic-scale Surface Science Research Center in Yonsei University, Korea. The XPS measurements were performed using a 300 mm diameter hemispherical energy analyzer with a multichannel detector. The pass energy of the energy analyzer was 23.5 eV. Monochromatized Al Kα X-rays (1486.6 eV) were used as the X-ray source. In addition, the current–voltage measurements

were carried out by using Keithley 236 source-measure unit and the EL was detected by a photodiode array.

3. Calculation details

To compare the calculations for a single molecule of the model and experiments on a solid, we must shift each computed vertical ionization potential (VIP), I'_k by a quantity WD illustrated by $I_k(\mathrm{EF}) = I'_k - \mathrm{WD}$. This fromula normalizes the ionization energy $I_k(\mathrm{EF})$ relative to the Fermi level. The quantity WD denotes the sum of the work function of the sample and other potential energy effects, which are described in previous studies [17–21].

3.1. Core-electron binding and emission energies and VIPs for XPS and XES

In order to obtain the accurate core-electron binding energies (CEBEs), we used the generalized transition-state (GTS) method. In the GTS method, Williams and co-workers [24] proposed the extension of Slater's transition-state method [22] and approximated the endothermicity $\Delta E = E(1) - E(0)$ by

$$\Delta E = [F(0) + 3F(2/3)]/4, \tag{1}$$

where $F(x) = \partial E(x)/\partial x$, and x $(0 < x \leqslant 1)$ is assumed to be a continuous variable, with $E(0)$ and $E(1)$ denoting the energies of the initial and final states, respectively. For example, for the ionization of an electron from molecular orbital (MO) ϕ_k of interest, x represents the fraction of electron removed, and, according to the Janak theorem [25], $F(x)$ is the negative orbital energy $\varepsilon_k(x)$. This procedure is applied in the following way. In the unrestricted GTS method, we removed 2/3 α electron from MO ϕ_k of interest.

For the VIPs of the valence regions, we use the so-called restricted diffuse ionization (rDI) model which Asbrink et al. [26] proposed in the HAM/3 method. In the rDI model, half of an electron is removed evenly from the valence MOs and the negative of the resulting orbital energies correspond to calculated VIPs. This allows us to obtain all the valence VIPs in a single calculation.

In the case of C and N Kα X-ray emission energy, we obtain the calculated values from the differences $[(\mathrm{CEBE})_{1s} - (\mathrm{VIP}, I_k)_{j[2p(A)]}]$ between CEBEs of the hole and VIPs of electrons to fill up the hole.

3.2. Intensity of XPS and XES

The intensity of valence XPS was estimated from the relative photoionization cross-section for Al Kα radiation using the Gelius intensity model [23]. For the relative atomic photoionization cross-section, we used the theoretical values from Yeh [27].

The XES intensity of carbon and oxygen spectral lines was obtained by summing the linear combination of atomic orbitals (LCAO) populations $P_{j[2p(A)]l}$ of the atomic orbitals $\chi_{2p(A)}(r)$ centered on given carbon and oxygen atoms; $l = x$, y and z.

In the case of C Kα and N Kα spectra the XES transition arises from outer occupied p orbitals to s-type holes in a given atom, due to the selection rule $\Delta l = \pm 1$. The intensity can be written as

$$I_{ij} \propto \left| \int \phi_i^{c}(r)(er)\phi_j(r)\,\mathrm{d}\tau \right|^2 = N_0 \left| \sum_{A} \int \chi_{1s(A)}(r)(er) \sum_{p(A)} C_{jp(A)}\chi_{(A)}(r)\,\mathrm{d}\tau \right|^2, \tag{2}$$

where $\phi_i^{c}(r)$ and $\phi_j(r)$ is a core hole and an outer valence MO, respectively. N_0 denotes a normalization factor, and $C_{jp(A)}$ is the LCAO coefficient of the atomic orbital $\chi_{p(A)}(r)$ centered on atom A. In order to calculate each intensity of XES for model molecules at each emission energy, we used the STO-3G basis set for each atom of the model molecules.

Considering the dipole selection rule and neglecting the terms involving orbital products on different atoms, an approximate intensity $I_{1s(A)j}$ is given by

$$I_{1s(A)j} = N'_0 \sum_{A} |C_{j[2p(A)]l}|^2, \tag{3}$$

where N_0' is a normalization factor, which includes the units of atomic dipole intensities. Thus, the XES intensity of carbon, and oxygen spectral lines was obtained by summing the LCAO populations of the atomic orbitals $\chi_{2p(A)}(r)$ centered on given carbon, and oxygen atoms; $l = x$, y and z.

DFT calculations of TPD were performed using a model monomer $(H_3CC_6H_4)N(C_6H_5)[C_6H_4CH{=}CH_2)]$ containing 41 atoms including 21 carbon atoms, a nitrogen atom and 19 hydrogen atoms for a total of 152 electrons, and 76 occupied orbitals to simulate the molecular structure of this compound shown in Fig. 1. The DeMon DFT program [13] was used for the calculations. For the geometry of the molecule, we used the optimized cartesian coordinate from the semiempirical AM1 (version 6.0) method [28]. The DeMon calculation was performed with the exchange-correlation potential labeled as B88/P86, made from Becke's 1988 exchange functional [29] and Perdew's 1986 correlation functional [30]. In the program, we used a nonrandom grid and polarized valence double-ς (DZVP) basis of $(621/41/1^*)$ for C and N, (41) for H with auxiliary fitting functions labeled (4, 4; 4, 4) for C and O, (3, 1; 3, 1) for H. In order to calculate each intensity of valence XPS and XES for model molecules, we considered only the atoms of the model molecule in the brace. We also used the STO-3G basis set for each atom of the model molecules to calculate the intensity of XES.

To simulate the valence XPS and XES of the TPD theoretically, we constructed from a superposition of peaks centered on each VIP, I_k and each emission energy, $[(CEBE)_{1s} - (VIP, I_k)_{j[2p(A)]}$, or $(CEBE)_{2p} - (VIP, I_k)_{j[3s(B)]}]$, respectively. As was done in previous work [17–21] each peak was represented by a Gaussian curve, and we used the line widths, $WH(k) = 0.10\ I_k$ (proportional to the ionization energy) and $WH(k) = 1.3$ eV (experimental resolution) for valence XPS and XES, respectively.

4. Results and discussion

4.1. Electroluminescence properties

To elucidate the effect that organic TPD layers might have on the EL, we prepared the OLEDs, such as Al(200 nm)/Alq_3(60 nm)/TPD(50 nm) on ITO glasses by ICBD and NCBD, respectively. The device with the same geometry by thermal evaporation was also prepared for comparison. Fig. 2 shows the EL results of our samples. The luminescence intensity of an OLED prepared by the ICBD method is about 10 times larger (starting at about 8 V) compared to the device prepared by the conventional thermal evaporation. The sample prepared by the NCBD technique has an onset that occurs at higher bias and therefore has insignificant luminescence in the bias region of importance. In the EL process, the TPD layer has been known to play a role as transport layer for holes in the OLEDs, because the TPD layer blocks electrons injected from the metal electrode and transports holes only. The luminescence efficiency of the device is influenced by the quality of TPD layer and the chemical structure of the TPD layers is a very important property.

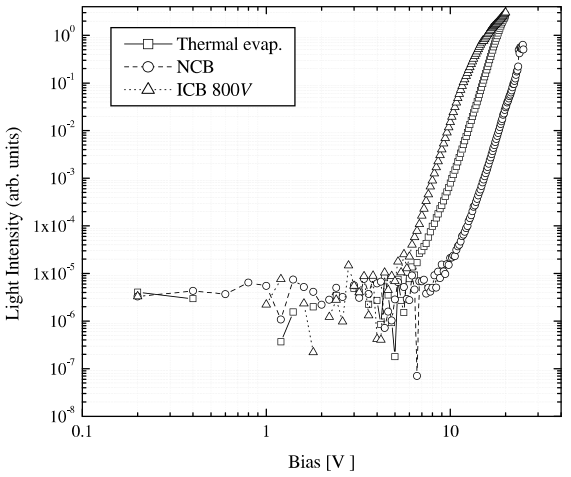

Fig. 2. EL spectra of organic electroluminescent devices: Al(200 nm)/Alq_3(60 nm)/TPD(50 nm) on indium-tin-oxide glasses.

4.2. X-ray fluorescence measurements

Soft X-ray emission spectroscopy is governed by the dipole selection rules and it can be used to study the local bonding environment of a sample. XES site-selectively probes the symmetry restricted valence states and it can be directly compared

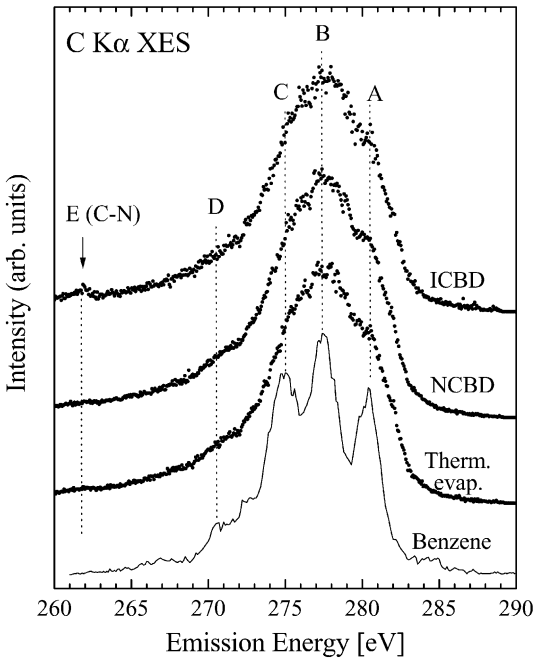

Fig. 3. C Kα XES of TPD films.

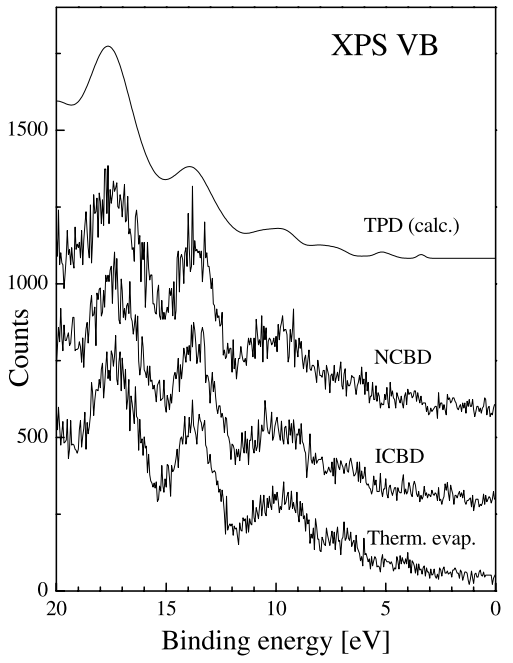

Fig. 4. Experimental and calculated XPS VB of TPD films (the calculated spectrum is shifted to 3.0 eV).

to MO calculations. The electronic transitions are limited to the first coordination sphere of the emitting atom, making the technique sensitive to short-range order (coordination number, bond length, etc.).

Fig. 3 displays the Carbon Kα emission ($2p \rightarrow 1s$ transitions) of TPD. The fine structure in the spectra is due to the overlapping peaks labeled A through E. The energetic positions of the peaks of TPD films coincide with those of benzene [31], because phenyl groups are mainly contributing to the formation of the structure of TPD as well (see Fig. 1). The spectra are found to be different with respect to the presence of the smallest peak labeled as E at about 262 eV. This peak is present only for the film prepared by ion cluster beam deposition. In order to discuss these changes in the spectra of TPD films one has to analyze the details of the electronic structure of TPD.

4.3. Density-functional theory calculations

The DFT calculations were performed for the model monomer $(H_3CC_6H_4)N(C_6H_5)[C_6H_4CH{=}CH_2)]$. To check the validity of these calculations we have compared the experimental and calculated XPS VB of TPD on a binding energy scale in Fig. 4. The calculations and experiment show the same structure and are in good agreement. The most intense experimental peak centered at 17.5 eV corresponds to the ionization of $\{s_\sigma(C\,2s–C\,2s)\text{-}B\}$ bonding orbitals which result from the –Ph (phenyl) and $–CH_3$ functional groups of TPD. The next peak located at about 13.6 eV is assigned to contributions from $\{p_\sigma(C\,2p–C\,2s), p_\sigma(N\,2p–C\,2s)\}$ bonding orbitals from –Ph and C–N functional groups, respectively. A third peak centered around 10 eV is due to $p_\sigma(C\,2p–C\,2s)$ bonding orbitals from –Ph functional groups. The next two peaks at 7.3 and 6.7 eV are due to $p_\sigma(C\,2p–N\,2p, C\,2p)$ and $p_\pi(C\,2p–C\,2p)$ bonding orbitals from –C–N and –Ph groups, respectively. We attribute the peak located at about 4.0 eV to N 2p lone pair non-bonding orbitals. Table 1 gives an overview of the energy positions of the observed XPS valence band peaks, the calculated VIPs, the main atomic orbitals, and the orbital nature and the corresponding functional groups of the TPD films. We note that

Table 1
Energy position of observed peaks, VIP (in eV), main atomic orbitals, orbital nature and functional groups from calculation and XPS measurement of TPD (calculated VIPs shifted by 3.0 eV)

Observed peaks (eV)	VIP (eV)	Main atomic orbital	Orbital nature	Functional group
	23.5	N 2s (0.8), C 2s (0.2)	s_σ(N 2s–C 2s)-B	N–C
	20.4, 20.3, 19.9	C 2s	s_σ(C 2s–C 2s)-B	–Ph
17.5	18.1–16.4, 15.7	C 2s	s_σ(C 2s–C 2s)-B	–Ph, CH_3
13.6	14.7–12.9, 12.6	C 2p, C 2s (0.8)	p_σ(C 2p–C 2s)-B	–Ph
		N 2p (0.8)	p_σ(N 2p–C 2s)-B	C–N
10.6–9.3	11.2–9.4	C 2p, C 2s	p_σ(C 2p–C 2s)-B	–Ph
7.3	8.4–8.0	C 2p (0.5), N 2p (0.5)	p_π(C 2p–N,C 2p)-B	C–N, –Ph
	7.7–7.0	–C 2p	p_π(C 2p–C 2p)-B	–Ph
6.7	6.8–6.0	C 2p (0.4), N 2p (0.6)	p_π(C 2p–N,C 2p)-B	C–N, –Ph
4.0	3.4	N 2p	p_π(lone pair)-NB	N

noticeable changes in the fine structure of the experimental XPS VB of different TPD films were not detected owing to the lack of bulk sensitivity of XPS VB in comparison to XES.

Fig. 5 is a comparison between the calculations and the Carbon Kα emission measured for the sample prepared by ICBD. Experiment and theory agree well. The results of our calculations are given in Table 2. We can assign the main experimental

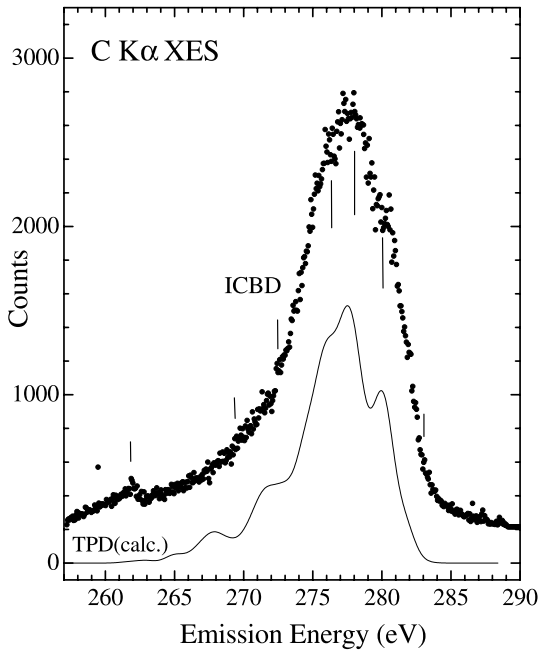

Fig. 5. Comparison of experimentally measured and theoretically calculated C Kα XES of TPD films.

Table 2
Energy positions of observed C Kα peaks, calculated emission energy, orbital nature and functional groups from calculation and XES measurement of TPD

Observed peaks (eV)	Emission energy (eV)	Orbital nature	Functional group
262	263.6	p_σ(C 2p–N 2s)-B	C–N
269–273	269.1–271.4	p_σ(C 2p–C 2s)-B	–Ph, CH_3
273–276	272.5–274.2	p_σ(C 2p–C 2s)-B	–Ph
276–280	276.0–277.8	p_π(C 2p–C 2p)-B	–Ph
	278.8–279.2	p_π(C 2p–C, N 2p)-B	–Ph, C–N
280–283 (shoulder peak)	281.8–282.5	p_π(C 2p–C 2p)-B	–Ph

C Kα XES peaks located in the energy range around 271–283 eV to p_σ(C 2p–C 2s) and p_σ(C 2p–C 2p) bonding orbitals of –Ph groups. The weak feature located at 262 eV is due to p_σ(C 2p–N 2s) bonding where three carbons bond directly to nitrogen and this feature indicates the existence of direct C–N bonding in TPD. Taking into account the experimental finding from Fig. 3 that this peak is clearly present only for the sample prepared by ICBD, it can be concluded that the number of C–N bonds is decreased in TPD films prepared by NCBD and by thermal evaporation. It is not clear at the moment why breaking some C–N bonds in the TPD structure leads to weakened EL in OLED devices. This phenomenon needs further investigations for clarification. In this paper we would like to emphasize the very high sensitivity XES has to local chemical bonding, which is an important

element for the characterization of polymer materials. XPS VB is less sensitive to the local chemical bonding and it is not surprising that we did not find any noticeable changes in these spectra for TPD films as a function of preparation conditions.

5. Conclusions

X-ray emission and photoelectron measurements of TPD films prepared by ICBD, NCBD and by thermal evaporation are presented. The obtained results are compared with our DFT calculations of the TPD monomer and the electronic structure of this material is discussed in detail. The X-ray fluorescence measurements suggest that the ICBD technique appears to be the best way for obtaining high quality TPD films with intense EL. For films prepared by NCBD or thermal evaporation some of C–N bonds in the TPD structure are broken.

Acknowledgements

This work was supported by the Korea Science and Engineering Foundation (project no. 995-0200-008-2), the Russian Science Foundation for Fundamental Research (projects 00-15-96575) and NATO Collaborative Linkage Grant. Funding by the President's NSERC fund of the University of Saskatchewan is gratefully acknowledged. Partially support by NSF grant DMR 9801804 is gratefully acknowledged. The work at the Advanced Light Source at Lawrence Berkeley National Laboratory was supported by US Department of Energy (contract no. DE-AC03-76SF00098).

References

[1] J.H. Burroughes, D.D.C. Bradley, A.R. Brown, R.N. Marks, K. Mackay, R.H. Friend, P.L. Burns, A.B. Holmes, Nature 347 (1990) 539.
[2] S.T. Kim, D.H. Hwang, X.C. Li, J. Gruener, R.H. Friend, A.B. Holmes, H.K. Shim, Adv. Mater. 8 (1996) 979.
[3] D. Braun, A.J. Heeger, Appl. Phys. Lett. 58 (1991) 1982.
[4] C.W. Tang, S.A. VanSlyke, Appl. Phys. Lett. 51 (1987) 913.
[5] C. Adachi, T. Tsutsui, S. Saito, Appl. Phys. Lett. 55 (1989) 1489.
[6] C. Adachi, T. Tsutsui, S. Saito, Appl. Phys. Lett. 57 (1990) 531.
[7] J. Littman, P. Matric, J. Appl. Phys. 72 (1992) 1957.
[8] P.E. Burrows, S.R. Forrest, Appl. Phys. Lett. 64 (1994) 2285.
[9] C. Hosokawa, H. Higashi, H. Nakamura, T. Kusumoto, Appl. Phys. Lett. 67 (1995) 3853.
[10] J.R. Sheats, H. Antoniadis, M. Hueschen, W. Leonard, J. Miller, R. Moon, D. Roitman, A. Stocking, Science 273 (1996) 884.
[11] A.J. Epstein, Y. Yang (Eds.), Polymeric and Organic Electronic Materials and Applications, MRS Bull. 22 (6) (1997) 13.
[12] K.W. Kim, S.C. Choi, S.S. Kim, S.J. Cho, C.N. Whang, H.S. Choe, H.J. Jung, D.H. Lee, J.K. Lee, J. Mater. Sci. 28 (1993) 1537.
[13] A. St-Amant, D.R. Salahub, Chem. Phys. Lett. 169 (1990) 387;
A. St-Amant, Ph.D. Thesis, University of Montreal, 1991.
[14] C.E. Hong, N.Y. Kim, S.Y. Kim, H.S. Yoon, K.W. Kim, C.N. Whang, Jpn. J. Appl. Phys. 36 (1997) 1715.
[15] C. Adachi, S. Tokito, T. Tsutsui, S. Saito, Jpn. J. Appl. Phys. 27 (1988) L269.
[16] J.J. Jia, T.A. Callcott, J. Yurkas, A.W. Ellis, F.J. Himpsel, M.G. Samant, J. Stöhr, D.L. Ederer, J.A. Carlisle, E.A. Hudson, L.J. Terminello, D.K. Shuh, R.C.C. Perera, Rev. Sci. Instrum. 66 (1995) 1394.
[17] K. Endo, Y. Kaneda, H. Okada, D.P. Chong, P. Duffy, Phys. Chem. 100 (1996) 19455.
[18] K. Endo, D.P. Chong, J. Surf. Anal. 3 (1997) 618.
[19] S. Kuroki, K. Endo, S. Maeda, D.P. Chong, P. Duffy, Polym. J. 30 (1998) 142.
[20] K. Endo, D.P. Chong, J. Surf. Anal. 4 (1998) 50.
[21] T. Otsuka, K. Endo, M. Suhara, D.P. Chong, J. Mol. Struct. 522 (2000) 47–60.
[22] J.C. Slater, Adv. Quant. Chem. 6 (1972) 1.
[23] U. Gelius, K. Siegbahn, Faraday Discuss. Chem. Soc. 54 (1972) 257;
U. Gelius, J. Electron Spectrosc. Relat. Phenom. 5 (1974) 985.
[24] A.R. Williams, R.A. deGroot, C.B. Sommers, J. Chem. Phys. 63 (1975) 628.
[25] J.F. Janak, Phys. Rev. A 18 (1978) 7165.
[26] L. Asbrink, C. Fridh, E. Lindholm, Chem. Phys. Lett. 52 (1977) 69.
[27] J.-J. Yeh, Atomic Calculation of Photoionization Cross Section and Asymmetry Parameters, Gordon and Breach Science Publishers, London, 1993.
[28] M.J.S. Dewar, E.G. Zoebisch, THEOCHEM 180 (1988) 1; M.J.S. Dewar, E.G. Zoebisch, E.F. Healy, J.J.P. Stewart, J. Am. Chem. Soc. 107 (1985) 3902.
[29] A.D. Becke, Phys. Rev. A 38 (1988) 3098.
[30] J.P. Perdew, Phys. Rev. B 33 (1986) 8822.
[31] P. Skytt, J. Guo, N. Wassdahl, J. Nordgren, Y. Luo, H. Agren, Phys. Rev. A 52 (1995) 3572.